Debye Length and Double-Layer Forces in Polyelectrolyte Solutions

Rafael Tadmor,[†] Ernesto Hernández-Zapata,[†,‡] Nianhuan Chen,[§] Philip Pincus,[⊥,#] and Jacob N. Israelachvili*[,†,§,#]

Materials Research Laboratory, University of California, Santa Barbara, California 93106; Instituto de Física, Universidad Nacional Autónoma de México, Apartado Postal 20-364, México DF 01000, Mexico; Department of Chemical Engineering, University of California, Santa Barbara, California 93106; Department of Physics, University of California, Santa Barbara, California 93106; and Biomolecular Science and Engineering, University of California, Santa Barbara, California 93106

Received October 31, 2001; Revised Manuscript Received January 5, 2002

ABSTRACT: We report experimental results and a theoretical analysis of the Debye length in aqueous solutions of nonadsorbing polyelectrolytes. The measurements were done using a surface forces apparatus, in which the normal forces between smooth mica surfaces in aqueous hyaluronic acid (HA) solutions were measured as a function of surface separation (to ±1 Å). HA is negatively charged and does not adsorb to the negatively charged surface of mica, as was established by optical and viscosity measurements and in agreement with the measured force−distance curves. From these measurements it appears that the multivalent polyelectrolyte is "depleted" from the gap between the surfaces. We use the mean-field Poisson−Boltzmann theory to theoretically predict the effective Debye length and double-layer force under such conditions and compare the predictions with the experimental results. The comparison gives excellent agreement and shows that the effective Debye length is determined solely by the monovalent ions in the solution. Specifically, the effective Debye length κ_{eff}^{-1} for the double-layer interaction is determined by an effective ionic concentration given by $\sqrt{n_s n_c}$, where n_s and n_c are the bulk negative and positive monovalent ion concentrations, respectively.

Introduction

When colloidal particles are dispersed in a medium containing free charges or ions (e.g., an aqueous electrolyte solution), the electrostatic interactions are screened by the free charges. The net "double-layer" interaction decays roughly exponentially with a characteristic length called the Debye length κ^{-1}. The Debye length is a crucial parameter in the description of aqueous systems that include ions, charged colloids, surfactants, polyelectrolytes, and biopolymers. Whereas the Debye length for simple electrolytes is well-known both theoretically and experimentally, that of more complex charged structures (polyelectrolytes, macroions, polysoaps, micelles, proteins) is still not well understood. Some experimental measurements have been made on the Debye length in micellar solutions;[1−3] however, for the case of surfaces immersed in polyelectrolyte solutions where the polymers cannot enter the gap between the surfaces, we could not find any theoretical or experimental study.

Polyelectrolytes in solution may be divided into adsorbing and nonadsorbing, each with its own unique features for the double-layer repulsion that it generates. The simplest of the two situations is the nonadsorbing polymer, since for adsorbing polymer we have in fact a problem of adsorbed *and* nonadsorbed polymers coexisting in the solution (since some polymer is always free in solution). We therefore chose to first investigate the case of nonadsorbing polymers, and for our model system we chose the sodium salt of hyaluronic acid (HA) as the polyelectrolyte, and mica surfaces. The electric double-layer forces between the mica surfaces were measured directly using the surface forces apparatus (SFA); the refractive index and viscosity of the solution confined between two mica surfaces were also measured. The HA−mica system was chosen because both are negatively charged so that HA does not adsorb on mica (in monovalent salt solutions such as NaCl and at physiological pH, i.e., near ∼7.0). HA is also an important natural (biological) polymer: it is found in certain body fluids such as synovial fluid (joint fluid) where it is believed to play a crucial role in biolubrication.

One may guess that for the interaction between two parallel surfaces a distance D apart in a solution of nonadsorbing macroions (say polyelectrolytes or micelles) there may be three regimes:

$$\text{(i) } D < \kappa_{\text{eff}}^{-1}$$

$$\text{(ii) } \kappa_{\text{eff}}^{-1} < D < mR_g$$

$$\text{(iii) } D > mR_g$$

where R_g is the dimension of the macroion in the solution, m is a constant of order unity, and κ_{eff}^{-1} is some effective Debye length for the double-layer interaction, where we assume that $\kappa_{\text{eff}}^{-1} < mR_g$. In regimes i and ii we expect the Poisson−Boltzmann (PB) equation to hold with some κ_{eff}^{-1}, while in regime iii the theories proposed by Borukhov et al.[4−6] (discussed later) hold. This study is focused on regime ii, where we expect the force between the surfaces to decay exponentially with the product $\kappa_{\text{eff}}D$. We predict the value of κ_{eff}^{-1} and measure it for the HA−mica system.

[†] Materials Research Laboratory, UCSB.
[‡] Universidad Nacional Autónoma de México.
[§] Department of Chemical Engineering, UCSB.
[⊥] Department of Physics, UCSB.
[#] Biomolecular Science and Engineering, UCSB.
* To whom correspondence should be addressed.

10.1021/ma011893y CCC: $22.00
Published on Web 02/16/2002

Experimental Section

Materials: Source and Preparation of HA Solutions. The HA (Sigma, H-9390) was the sodium salt of hyaluronic acid from *Streptococcus zooepidemicus* and was used as received. HA solutions were made in HEPES buffer: *N*-[2-hydroxyethyl]piperazine-*N*′-[2-ethanesulfonic acid] (Sigma, H-7523, used as received). 2.383 g/L of HEPES powder was titrated with NaOH solution to obtain a final solution of 4.13 mM Na^+ at pH 7.4. We refer later to this solution as "the buffer". HA is then dissolved in the buffer solution to a concentration of 3.4 mg/mL.

Materials: Characterization of HA Solutions. The molecular weight of the HA was obtain by comparing intrinsic viscosity measurements that we made in 0.1 M NaCl solution of our HA with those of Fouissac et al.[7] From these measurements,[8] the average molecular weight M and the average radius of gyration R_g of the HA used in this study were found to be $M = 540$ kDa and $R_g = 64$ nm, respectively. The Mark−Houwink−Sakurada equation in this case takes the form[8] $[\eta] = 0.0046M^{0.8}$, where $[\eta]$ is the *intrinsic* viscosity in mL/g and M is in daltons. The polydispersity in the molecular weight for this type (source) of HA is usually between 1.8 and 2.5.[9]

Methods: the Surface Forces Apparatus (SFA) Technique. Force measurements were done using a SFA Mark III.[10] The principles of the SFA technique have been extensively described.[10,11] Briefly, the shapes of and separation D between two smooth mica surfaces are measured during force measurements with an optical technique[12] having a distance resolution of ±1 Å. The optical technique also allows for the refractive index of the solution between the surfaces to be directly measured, which indirectly gives the density of dissolved polymer in the confined film between the surfaces. This may be quite different from the bulk value when the surfaces are close together (usually for films thinner than a few R_g).

The upper surface is mounted on a piezoelectric tube which allows control of the normal separation and motion (fine distance control to ±1 Å), and the lower surface is mounted on a weak cantilever spring, which can be moved normally from millimeters to nanometer separations (coarse distance control). From the deflection of this spring the normal force F between the two surfaces can be measured simultaneously with their separation D. The forces in this study are normalized by the radius $R \sim 20$ mm of the curved surfaces (which for convenience are arranged in the "crossed cylinder configuration"), since according to the Derjaguin approximation,[13] for $D \ll R$ the measured force F is related to the interaction energy per unit area E between two plane-parallel surfaces at the same separation D according to

$$E(D) = F(D)/2\pi R \tag{1}$$

Thus, normalizing the measured force-law $F(D)$ by the radius R enables comparison between different experiments as well as with theory which normally predicts $E(D)$. The way F/R varies with D is often referred to as the "force profile".

Results

Thin-Film Refractive Index and HA Concentration Measurements. To interpret the measured forces (and Debye length), we needed to establish whether the polymer is adsorbing or nonadsorbing. This was done in two ways: via refractive index and thin-film viscosity measurements. First, using an Abbé refractometer, the refractive index of the pure bulk buffer solution was found to be $r_s = 1.333$, the same as for pure water. The refractive index increment dr/dc (where c is the polymer concentration) of the HA solution in the buffer was found to be 0.143 mL/mg, which is similar to previous reports for other aqueous HA solutions.[14]

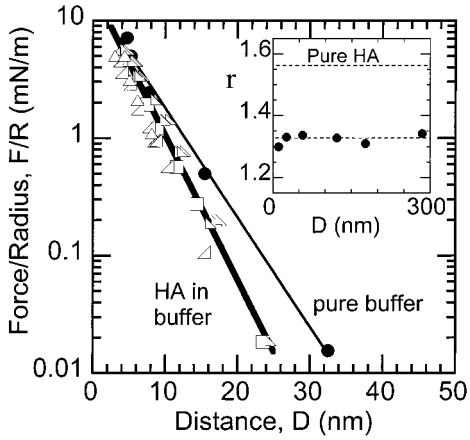

Figure 1. Measured forces between two mica surfaces across buffer solution (●) and across 3.4 mg/mL of HA in the buffer solution (△, right tilted △, left tilted △, □). The different symbols represent different force runs. The thinner solid line is the theoretical prediction for the buffer solution based on eqs 3 and 4b, and the thicker solid line is the theoretical prediction for the HA in buffer solution, using eqs 26 and 28, both based on the experimental concentrations. The inset shows the refractive index r of the confined HA/buffer solution vs the separation D between the mica surfaces.[8] The upper dashed line is the refractive index of pure HA, and the lower dashed line is the refractive index of the bulk solution (which is almost identical to the buffer solution). Both dashed line values were obtained using an Abbé refractometer.

An amorphous HA melt at room temperature (without solvent) has a refractive index r_p given by (see p 309 in ref 15)

$$r_p = r_s + \xi \frac{dr}{dc} \tag{2}$$

where ξ is the melt HA density in mg/mL. From eq 2 we obtain $r_p = 1.563$ for the refractive index of bulk amorphous HA, which is very close to the evaluation based on a theoretical correlation (see Chapter 10 in ref 15), which gives $r_p = 1.57$. By measuring the mean refractive index of the confined (nonbulk) solution between the surfaces in the SFA experiments, it was possible to determine the mean concentration c of HA in the gap (using eq 2) and, therefore, whether this was higher or lower than in the bulk "reservoir". If the refractive index is measured as a function of the confining separation D, this method may also provide a reasonably accurate way of measuring the amount of surface adsorbed material.[16−18]

The measured refractive index of a dilute, 3.4 mg/mL, HA solution as a function of the separation between two mica surfaces is shown in the inset in Figure 1. At large separations (thick films) the refractive index is, as expected, the same as the bulk value, which is indicated by the lower horizontal dashed line in the inset. As the separation between the mica surfaces is decreased, the refractive index remains the same as that for the bulk and does not increase toward the refractive index of pure HA (upper horizontal dashed line in the inset). This shows that the HA does not adsorb on the mica surface; i.e., it behaves as a "nonadsorbing" or "nonadhering" polyelectrolyte, which (as described below) is also consistent with the viscosity and force measurements.

Thin-Film Viscosity. A clear manifestation for the depletion of the polymer from between the surfaces is deduced from the viscosity measurements which are

reported in ref 8. The viscosity was measured by vibrating one of the surfaces sinusoidally (in the vertical direction) and measuring the resulting sinusoidal change in the surface separation. The viscosity profile was then calculated as explained in ref 19.

The viscosity measurements[8] show that at large separations, $D > 6R_g$, the viscosity is the same as that of the bulk solution (ca. 22.5 cP) as measured using a U-tube capillary viscometer. However, as the separation between the surfaces is decreased to below about 400 nm, the viscosity starts to decrease monotonically until, at about 20 nm, corresponding to $D \approx {}^1/_2R_g$, it reaches a value of only ~2.5 cP. This drastic decrease in the viscosity shows (as do the refractive index measurements and normal force profiles—to be reported in the next paragraph) that the polymer is depleted from the gap.

Normal Force Profiles. The measured force profile $F(D)/R$ between two mica surfaces across pure buffer solution (no HA added) is shown by the solid circles in Figure 1. This can be fitted to the theoretical approximate expression for the exponentially decaying electrostatic double-layer repulsion in monovalent electrolyte solution, given by[20,21]

$$\frac{F}{R} = \frac{128\pi n_s k_B T}{\kappa} \tanh^2\left(\frac{e\psi_0}{4k_B T}\right) e^{-\kappa D} \qquad (3)$$

where n_s is the bulk salt concentration in units of number density (m^{-3}), k_B is the Boltzmann constant, T is the temperature, ψ_0 is the surface electrostatic potential, e is the electronic charge, and κ^{-1} is the Debye screening length, given by

$$\kappa^{-1} = [\epsilon\epsilon_0 k_B T / \sum_i n_i z_i^2 e^2]^{1/2} \qquad (4a)$$

where n_i and z_i are the concentration and valency of the ith ion species (in units of number density), ϵ is the dielectric constant of water, and ϵ_0 is the permittivity of free space. For monovalent electrolytes (which will be discussed further on in this study) this reduces to

$$\kappa^{-1} = [\epsilon\epsilon_0 k_B T / 2n_s e^2]^{1/2} \qquad (4b)$$

Equation 3 is valid for D larger than the Debye length. The thin line in Figure 1 is the best exponential fit to the measured double-layer force in the pure hepes buffer (at pH 7.4). The fit gives a Debye length of $\kappa^{-1} = 4.7 \pm 0.1$ nm. From eq 4b this corresponds to a monovalent salt concentration of $n_s = 4.1$ mM, which is in full agreement with the known concentration of 4.13 mM of the buffer solution. From eq 3 the fitted surface potential is $\psi_0 = -150$ mV, which, using the Grahame equation,[22] corresponds to a surface charge density of $\sigma = 0.071$ C/m^2 (equivalent to one electron charge per 2.3 nm^2).

To this buffer solution HA was added, bringing it to a concentration of $c = 3.4$ mg/mL (6.8×10^{-3} mM). In this polymer solution the measured forces are again exponentially repulsive, as shown in Figure 1 (open symbols) for four different runs. But this time we do not know in advance what to expect for the Debye length—especially the contribution from the added polyelectrolyte. Assuming that eq 3 still holds, the measured (fitted) Debye length is now smaller than for the buffer solution without HA: the average value obtained from fitting eq 3 to the four independently measured force profiles in the HA solution is $\kappa_{eff}^{-1} = 3.5 \pm 0.1$ nm (compared to 4.7 nm in the pure buffer). Qualitatively, the decrease in the Debye length is expected from the increase in the ionic concentration as a result of the addition of dissociated HA. To account for this effect quantitatively, we describe below a simple model for predicting the effective Debye lengths in nonadsorbing polyelectrolyte and other macroionic solutions.

Discussion and Theory

We first discuss some important experimental and system-specific features that a general model of the Debye length must consider. The Debye length κ^{-1} is defined by eq 4a solely in terms of the bulk properties of the solvent or suspending medium, viz., its dielectric constant, temperature, and the valency and concentration of added inert (i.e., overall electrically neutral) electrolyte ions.

In the case of "zero salt", when there are no inert electrolyte ions in the reservoir, or in the case of highly concentrated colloidal dispersions, the ions present in the solution are mainly the counterions that have come off (dissociated from) the particle surfaces. The bulk reservoir no longer consists of a fixed concentration of inert (electroneutral) electrolyte, and the Debye length should also depend on the concentration and charge of the solute particles in the solvent. Dubois et al.[23] have presented a unified theory of double-layer interactions that covers all situations—from "excess inert electrolyte" to "counterions only".

In the present case we have a system that is yet more complex: charged surfaces interacting in a solvent containing both inert electrolyte ions and a charged polyelectrolyte macroion and where neither the concentration of the salt electrolyte ions nor the polyelectrolyte counterions in the reservoir can be neglected. In addition, the nature of the surface forces is such that the polyelectrolyte is forced out from between the surfaces as they approach each other already from a large separation. The question is, what is the definition and meaning of the Debye length in such systems or situations, and how is it involved in the interaction between charged surfaces? The case when the polymers are not forced out from the gap (i.e., at large distances) was studied by Borukhov et al.[6] They obtained a modified PB equation and calculated the polymer concentration profile between the surfaces. In subsequent studies,[4,5] the same authors investigated confined macroions (rather than polymers) and developed yet another modified PB equation. Indeed, the Debye length obtained from the linear approximation of their modified PB equation is the same as if the macroions were considered as points with charges that correspond to their valency (see also ref 24).

In one of the few quantitative experimental measurements on a system of this kind, Pashley and Ninham[2] measured the double-layer forces between surfaces of adsorbed cationic cetyltrimethylammonium bromide (CTAB) bilayers across a micellar solution of CTAB above the critical micelle concentration (cmc). The solution contained isolated dissociated surfactant molecules of cetyltrimethylammonium acid (CTA^+), their counterions of Br^-, micelles of diameter ~30 Å consisting of about 50 CTAB surfactant molecules, of which ~25% were dissociated, and the micelle counterions of

Br^-. The effective Debye length was 6 nm, as ascertained from the fitted exponential decay of the double-layer force in the range ~0−26 nm, i.e., including separations that are larger than both the micelle size and effective Debye length. This value was empirically found to be close to the standard expression for κ^{-1}, eq 4a, but with only the small monovalent ions contributing to $\sum_i c_i z_i^2$. This suggested that the charged micelles, in contrast to their dissociated counterions, were not contributing to the Debye length, but no attempt was made to theoretically explain this interesting effect.

In our experiments of nonadsorbing HA between similarly charged mica surfaces in monovalent inert electrolyte solution, an effective Debye length of 3.5 nm was measured in the distance range 3−25 nm, i.e., at distances larger than the Debye length but *smaller* than the size of the macroions whose radius of gyration was ~64 nm. Indeed, as shown in Figure 1, whenever a force was detected, it was in the range where $D \ll R_g$ where it was unfavorable for the polymers to remain in the gap between the surfaces (discussed in the next paragraph). Thus, we assume that at these separations the amount of polymer in the gap is negligible. One may argue that since the surfaces are rounded, then way off the closest approach there will still be a considerable amount of polymer; however, way off the closest approach the separation becomes so large that the double-layer contribution to the net force is negligible.

Modeling the Effective Debye Length. We first give a qualitative theoretical justification for our assumption (supported by our experimental observation[8]) of no polymer in the gap. The ejection (depletion) of polymer from a confined space into the bulk reservoir results from two opposing effects: the resulting *decrease* in the translational entropy, S_{trans}, which is proportional to the number of depleted polymer molecules p, and the *increase* of their conformational entropy, S_{conf}, which is proportional to Np, where N is the degree of polymerization (number of segments per molecule). Since $N \gg 1$, then $S_{conf} \gg S_{trans}$, and the polymer will be depleted from the gap. Additionally, since both our polymer and the surfaces are negatively charged, there is also an electrostatic repulsion, which contributes to the depletion. We therefore adopt the "no polymer in the gap" assumption as a reasonable approximation in our model for the Debye length of nonadsorbing polymer.

To discuss the contribution to the effective Debye screening length due to dissolved but nonadsorbing polymer, we must also consider the energy and entropy associated with its inability to be in the gap. We first consider the very simple system of two identical parallel infinite planes with equal surface charge density $-\sigma$ at positions $X = 0$ and $X = D$ (Figure 2). In the space between the planes there is an aqueous solution containing two kinds of ions: negative monovalent salt ions (from the buffer) with number concentration $n_s(X)$ and positive monovalent ions with number concentration $n_c(X)$ which include the ions from the buffer, the mica surfaces, and the polymer. The polymer itself is excluded from the gap. For simplicity, we assume all the monovalent ions to be point charges. The regions outside the gap ($X < 0$ and $X > D$) are occupied by the substrate and are therefore free of solution and charges.

The system is in contact with a bulk reservoir with given ion concentrations: n_s for the monovalent anions (the concentration in the buffer solution), n_c for the monovalent cations, and n_p for the macroions (the HA

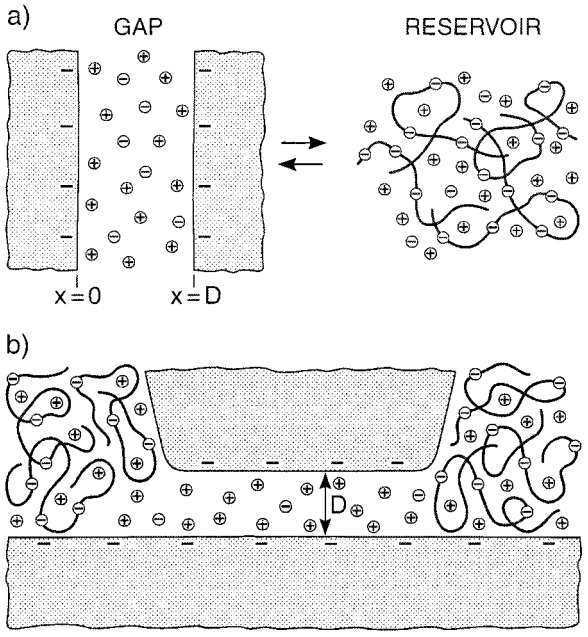

Figure 2. A schematic of the model system used for the theoretical derivation of the effective Debye length. (a) The left-hand side represents the solution in the gap between the mica surfaces, and the right-hand side represents the bulk solution (reservoir) which is in equilibrium with the solution in the gap. The polymers—shown as coils on the right—are not allowed inside the gap while the monovalent ions are. The real system that the model describes may look more like (b) provided that the lateral dimension of the upper surface is much larger than the separation D between the surfaces.

polymer concentration). Because of charge neutrality, the equation

$$n_c = n_s + Zn_p \tag{5}$$

must be satisfied in the reservoir, where Z is the number of elementary charges per polyelectrolyte chain. (The concentration of the counterions from the mica surfaces is zero in the reservoir.) We assume that the distance between charges along the polymer chain for HA is bigger[25−31] than the Bjerrum length (~7 Å); therefore, we expect no Manning counterion condensation[32−35] in our system, and the valency Z of the polyelectrolyte does not have to be renormalized. The effect of the polyelectrolyte on the properties of the solution inside the gap is indirect, through the fixing of the chemical potential of the monovalent species.

Since the system is symmetric, we just need to solve the problem for the region $0 < X < D/2$. We write an expression for the grand potential (grand canonical potential[36]) functional Ω per unit area A:

$$\frac{\Omega}{Ak_BT} = 2\int_0^{D/2} dX \left\{ n_c(X)(\ln[\varsigma^3 n_c(X)] - 1) + n_s(X)(\ln[\varsigma^3 n_s(X)] - 1) + \frac{1}{2}\phi(X)[n_c(X) - n_s(X) - \sigma\delta(X)] - \frac{\mu_c}{k_BT} n_c(X) - \frac{\mu_s}{k_BT} n_s(X) + \frac{\Pi_0}{k_BT} \right\} \tag{6}$$

The first two terms in the integral represent the ideal-solution entropy of the mobile monovalent ions. The third term represents the electrostatic interactions due

to the charge distribution in the system, $\phi(X) = e\psi(X)/k_BT$ is the reduced (dimensionless) electrostatic potential, ς is an (irrelevant) length scale that represents the monovalent ion dimensions, and Π_0 is the reference external pressure corresponding to the semidilute polyelectrolyte solution in the reservoir. The electrochemical potentials were set to $\mu_c = k_BT \ln(\varsigma^3 n_c)$ and $\mu_s = k_BT \ln(\varsigma^3 n_s)$ for the negative and positive monovalent ions, respectively. These values for the chemical potentials assume a dilute reservoir, for which the ideal-solution expression applies. Please note that n_c and n_s are *not* the same as $n_c(X)$ and $n_s(X)$: the first two are the constant concentrations at the bulk, and the last two are the varying concentrations between the surfaces.

The expression for the electrostatic potential corresponding to a charge distribution that depends on just one dimension (X in the present case) is

$$\phi(X) = -\left(\frac{2e^2}{\epsilon\epsilon_0 k_B T}\right)\int_0^D dX' \, |X - X'|[n_c(X') - n_s(X') - \sigma\delta(X') - \sigma\delta(X' - D)] \quad (7)$$

It is easy to see that $\phi(X)$, eq 7, satisfies the Poisson equation:

$$\frac{d^2\phi(X)}{dX^2} = -\frac{e^2}{\epsilon_0\epsilon k_B T}[n_c(X) - n_s(X)] \quad (8)$$

If we now substitute the expressions for the chemical potentials in eq 6 and rearrange, we get

$$\frac{\Omega}{2Ak_BT} = \int_0^{D/2} dX \left\{ n_c(X) \ln[n_c(X)/n_c] + n_s(X) \ln[n_s(X)/n_s] - \left[n_c(X) + n_s(X) - \frac{\Pi_0}{k_BT}\right] + \frac{1}{2}\phi(X)[n_c(X) - n_s(X) - \sigma\delta(X)] \right. \quad (9)$$

The electrolyte concentrations are subjected to the restriction of global charge neutrality:

$$F[n_c(X), n_s(X)] \equiv \int_0^{D/2}[n_c(X) - n_s(X) - \sigma\delta(X)] \, dX = 0 \quad (10)$$

The integration is between $X = 0$ and $X = D/2$ because the system is symmetric with respect to $D/2$, and then one charged surface should be neutralized by the charges of the free ions in half of the space between the plates.

At the mean-field level, the equilibrium ion concentrations for pointlike charges are obtained by minimizing the grand-potential functional, eq 9, with respect to the ion densities, taking into account the restriction of global charge neutrality, eq 10, that is, $(\delta/\delta n_c(X))[\Omega/2Ak_BT] = \lambda(\delta F/\delta n_c(X))$ and $(\delta/\delta n_s(X))[\Omega/2Ak_BT] = \lambda(\delta F/\delta n_s(X))$, where λ is a Lagrange multiplier. Following this procedure (see the Appendix), we obtain the Boltzmann distributions in the form

$$n_s(X) = n_s \exp[\phi(X) - \lambda]$$
$$n_c(X) = n_c \exp[-\phi(X) + \lambda] \quad (11)$$

Defining $\exp[\phi^*] \equiv \sqrt{n_s/n_c}$, $\bar{\phi}(X) \equiv \phi(X) + \phi^* - \lambda$, and the effective salt concentration inside the gap as

$$n_{eff} \equiv \sqrt{n_s n_c} \quad (12)$$

we may now rewrite eq 11 in the following way:

$$n_s(X) = n_{eff} \exp[\phi(X) + \phi^* - \lambda] = n_{eff} e^{\bar{\phi}(X)}$$
$$n_c(X) = n_{eff} \exp[-\{\phi(X) + \phi^* - \lambda\}] = n_{eff} e^{-\bar{\phi}(X)} \quad (13)$$

For sufficiently long separations D between the plates, there is approximate local charge neutrality at the midplane ($X = D/2$), so we have in that case $n_s(D/2) \cong n_c(D/2)$. This leads to $\bar{\phi}(D/2) = \phi(D/2) + \phi^* - \lambda = 0$, according to eq 13 and, therefore, $n_s(D/2) \cong n_c(D/2) \cong n_{eff}$. It is therefore suggestive that this is indeed the physical magnitude that we should use instead of the ionic concentration to calculate the effective Debye length, viz.

$$\kappa_{eff}^{-1} = [\epsilon\epsilon_0 k_B T/2n_{eff}e^2]^{1/2} \quad (14)$$

It turns out that κ_{eff}^{-1} is intermediate between the Debye length prior to the introduction of the HA polymer, i.e., $\kappa^{-1} = \sqrt{\epsilon\epsilon_0 k_B T/2n_s e^2}$, as given by eq 4b, and the Debye length we would obtain if each polymer chain in the solution were substituted by Z monovalent ions that were allowed to enter into the gap, i.e., $\sqrt{\epsilon\epsilon_0 k_B T/2n_c e^2}$, where n_c is defined in eq 5.

Modeling the Double-Layer Interaction. Combination of eqs 8, 11, and 13 leads to the well-known Poisson−Boltzmann equation:

$$\frac{d^2\bar{\phi}(X)}{dX^2} = \frac{-e^2}{\epsilon\epsilon_0 k_B T}[n_c(X) - n_s(X)] = \kappa_{eff}^2 \sinh \bar{\phi}(X) \quad (15)$$

A first integration of eq 15 leads to the following formula for the electric field in the region $0 < X < D/2$:

$$\frac{d\bar{\phi}}{dX} = \kappa_{eff}\Delta(\bar{\phi}(X); \bar{\phi}_d) \quad (16)$$

where $\Delta(\bar{\phi}(X); \bar{\phi}_d) \equiv \sqrt{2(\cosh\bar{\phi}(X) - \cosh\bar{\phi}_d)}$, $\bar{\phi}_d \equiv \bar{\phi}(D/2)$, and where we have used the relation $2\,d^2\phi/dX^2 = d[(\phi')^2]/d\phi$ and the fact that the electric field is zero at the midplane ($X = D/2$) because of the symmetry of the system.

A second integration leads to

$$\kappa_{eff}\frac{D}{2} = \int_{\bar{\phi}_0}^{\bar{\phi}_d} \frac{d\bar{\phi}}{\Delta(\bar{\phi}(X); \bar{\phi}_d)} \quad (17)$$

The boundary condition for the electric field at the mica surface ($X = 0$) combined with eq 16 leads to

$$\kappa_{eff}\Delta(\bar{\phi}_0; \bar{\phi}_d) = \frac{d\bar{\phi}}{dX}(0) = \frac{e^2}{\epsilon\epsilon_0 k_B T}\sigma \quad (18)$$

Equations 17 and 18 determine $\bar{\phi}_0 = \bar{\phi}(0)$ and $\bar{\phi}_d = \bar{\phi}(D/2)$ for any given separation D. Substituting eq 13 in eq 9 and using eqs 16 and 17 leads to

$$-\frac{\Omega}{2Ak_BT} = 2n_{eff}D\sinh^2\frac{\bar{\phi}_d}{2} + 2\frac{n_{eff}}{\kappa_{eff}}\int_{\bar{\phi}_0}^{\bar{\phi}_d}\Delta(\bar{\phi};\bar{\phi}_d)\,d\bar{\phi} + \frac{n_{eff}}{\kappa_{eff}}(\bar{\phi}_0 - \phi^* + \lambda)\Delta(\bar{\phi}_0;\bar{\phi}_d) + \frac{\sigma\phi_0}{2} + \left[2n_{eff} - \frac{\Pi_0}{k_BT}\right]\frac{D}{2} \quad (19)$$

The disjoining osmotic pressure Π between the planes is given by the negative (total) derivative of the grand-potential (per unit area) with respect to the separation of the surfaces D. Therefore

$$\frac{\Pi}{2k_BT} = \frac{\partial}{\partial D}\left(-\frac{\Omega}{2Ak_BT}\right) = \frac{1}{2}\left(2n_{eff} - \frac{\Pi_0}{k_BT}\right) + 2n_{eff}\sinh^2\frac{\bar{\phi}_d}{2} + \left[\frac{\sigma}{2} - \frac{n_{eff}}{\kappa_{eff}}\Delta(\bar{\phi}_0;\bar{\phi}_d)\right]\frac{\partial\bar{\phi}_0}{\partial D} + \left[n_{eff}D\sinh\bar{\phi}_d - 2\frac{n_{eff}}{\kappa_{eff}}\int_{\bar{\phi}_0}^{\bar{\phi}_d}\frac{\sinh\bar{\phi}_d}{\Delta(\bar{\phi};\bar{\phi}_d)}\right]\frac{\partial\bar{\phi}_d}{\partial D} + \frac{n_{eff}}{\kappa_{eff}}\frac{(\bar{\phi}_0 - \phi^* + \lambda)}{\Delta(\bar{\phi}_0;\bar{\phi}_d)}\left(\sinh\bar{\phi}_0\frac{\partial\bar{\phi}_0}{\partial D} - \sinh\bar{\phi}_d\frac{\partial\bar{\phi}_d}{\partial D}\right) \quad (20)$$

The quantities in the two square brackets are zero because of eqs 17 and 18. The fifth term may also be shown to be zero by differentiating eq 18 with respect to D. So the osmotic pressure reduces to

$$\frac{\Pi}{k_BT} = 4n_{eff}\sinh^2\frac{\bar{\phi}_d}{2} + \left[2n_{eff} - \frac{\Pi_0}{k_BT}\right] \quad (21)$$

which may be expressed in a more familiar form as

$$\frac{\Pi}{k_BT} = n_s(D/2) + n_c(D/2) - \frac{\Pi_0}{k_BT} \quad (22)$$

Equation 21 or 22 is the version of the so-called "contact value theorem"[21,37,38] for our system. The term in the square brackets in eq 21 is the constant osmotic term, present even in the case of well-separated planes so long as the macroions are unable to enter the gap. This term is assumed to be small compared to the first term in the right-hand side of eq 21.

As was previously discussed, for sufficiently large separations ($D \gg \kappa_{eff}^{-1}$) the modified electrostatic potential in the midplane, $\bar{\phi}(D/2)$, is very small. Therefore, we may use the well-known weak overlap approximation,[11,20,21,39] which leads to

$$\frac{\Pi}{k_BT} \cong 64n_{eff}\tanh^2\left(\frac{\bar{\phi}_0}{4}\right)e^{-\kappa_{eff}D} \quad (23)$$

At low surface potentials ($|k_BT\bar{\phi}_0/e| < 25$ mV) eq 23 further simplifies to

$$\frac{\Pi}{k_BT} \cong \frac{2e^2\sigma^2}{\epsilon\epsilon_0k_BT}e^{-\kappa_{eff}D} \quad (24)$$

which can also be obtained from the linearization of the PB equation (15) by assuming $\sinh\bar{\phi}(X) \approx \bar{\phi}(X)$.

The disjoining osmotic pressure may now be reintegrated to obtain the interaction grand potential in the weak overlap approximation limit as

$$\frac{\Omega}{Ak_BT}(D) - \frac{\Omega}{Ak_BT}(\infty) \cong \frac{64n_{eff}}{\kappa_{eff}}\tanh^2\left(\frac{\bar{\phi}_0}{4}\right)e^{-\kappa_{eff}D} \quad (25)$$

where $\Omega/A(\infty)$ is the grand potential per unit area corresponding to the situation when the two planes are very far away from each other ($D \gg \kappa_{eff}^{-1}$). Finally, the ratio force/radius between two spheres, a sphere and a flat surface, or two crossed cylinders, F/R, as measured in the SFA experiments, would be proportional to the interaction grand potential (per unit area) as given by the Derjaguin approximation.[13,40] So for the case of two crossed cylinders (or a sphere near a flat surface) we may expect the following relation to apply:

$$\frac{F}{R} \cong 2\pi k_BT\left[\frac{\Omega}{Ak_BT}(D) - \frac{\Omega}{Ak_BT}(\infty)\right] \cong \frac{128\pi k_BTn_{eff}}{\kappa_{eff}}\tanh^2\left(\frac{e[\psi_p + \psi^*]}{4k_BT}\right)e^{-\kappa_{eff}D} \quad (26)$$

which is totally analogous to eq 3 with the substitution of κ by κ_{eff}, n_s by n_{eff}, and ψ_0 by $\psi_p + \psi^*$ where $\psi_p = \bar{\psi}_0 - \psi^*$ is the difference between the potentials at the surface and at the reservoir, $\psi^* \equiv (k_BT\phi^*/e)$, and $\bar{\psi}_0 \equiv (k_BT\bar{\phi}_0/e)$. Unlike in eq 3 where the difference between the potentials at the surface and at the reservoir is ψ_0, in the case described by eq 26 it is $\psi_p = \bar{\psi}_0 - \psi^*$. (Note that in eqs 11 and 13, when we use $\bar{\phi} = \phi^*$, we have $n_s(X) = n_s$ and $n_c(X) = n_c$ which are their values in the reservoir; hence, ψ^* is the value of the potential in the reservoir.) One way of explaining the difference in the potential used in eq 26 and that used in eq 3 is by considering a system of two well-separated parallel membranes in which the polymer can be only outside the gap between the surfaces. Although the surfaces are very far away, the surface potential is different if considered with respect to the midplane of the gap than it is with respect to the reservoir. This is because the system is not symmetric as opposed to the same system but without the polymer.

Summary and Conclusions

The electric double-layer forces between two mica surfaces across a monovalent salt solution with and without a nonadsorbing polyelectrolyte of the high molecular weight HA (5.4×10^5 Da, $R_g \approx 64$ nm) were measured. From these measurements, it was found that the effective Debye length at surface separation below R_g was reduced from 4.7 ± 0.1 nm in 4.1 mM salt to 3.5 ± 0.1 nm after addition of 6.8 μM HA.

The double-layer repulsion for a salt solution containing nonadsorbing polymer was also treated theoretically. It is shown that the effective Debye length in such systems is expected to be

$$\kappa_{eff}^{-1} = \left(\frac{n_s}{n_s + Zn_p}\right)^{1/4}\kappa^{-1} \quad (27)$$

where κ^{-1} is the Debye length in pure salt solution ($n_p = 0$). Equation 27 shows that addition of a nonadsorbing polyelectrolyte of concentration n_p and valency Z (i.e., additional counterion concentration of Zn_p) to an existing monovalent salt solution of concentration n_s changes the Debye length from κ^{-1} to κ_{eff}^{-1}. In terms

of molar concentrations for n_s and n_p, eq 27 may be written as

$$\kappa_{eff}^{-1} = \frac{0.304}{\sqrt[4]{n_s(n_s + Zn_p)}}\ \text{nm} \quad (28)$$

Using either eq 28 or eq 27, we may calculate the theoretically expected Debye length κ_{eff}^{-1} for our experimental system assuming fully dissociated polymer ($Z = N = 1250$). This calculation results in $\kappa_{eff}^{-1} = 0.304/[4.13 \times 10^{-3}(4.13 + 1250 \times 0.0068) \times 10^{-3}]^{1/4} = 3.53$ nm, which is in excellent agreement with the experimental Debye length of 3.5 ± 0.1 nm. The thick solid line in Figure 1 uses the (theoretical) value of 3.53 nm for κ_{eff}^{-1}.

From fitting eq 26 to the experimental data, we can also learn that addition of HA to the buffer solution resulted in a surface potential of $\bar{\psi}_0 = -125$ mV. The corresponding difference between the potentials at the surface and at the reservoir is given by

$$\psi_p = \bar{\psi}_0 - \psi^* = \bar{\psi}_0 - (k_B T/e)\ln\left(\frac{n_s}{n_s + Zn_p}\right)^{1/2} \quad (29)$$

which results in $\psi_p = -139$ mV. Thus, the surface potential (with respect to the reservoir) had decreased from $\psi_0 = -150$ mV to an effective potential of $\psi_p = -139$ mV on addition of HA.

Similarly, the effective surface charge density in the HA solution may be calculated using the Grahame equation,[22] which for our case becomes modified as follows:

$$\sigma = \sqrt{8\epsilon\epsilon_0 k_B T}\sinh(e\bar{\psi}_0/2k_B T)n_{eff}^{1/2} = \sqrt{8\epsilon\epsilon_0 k_B T}\sinh(e\bar{\psi}_0/2k_B T)[n_s(n_s + Zn_p)]^{1/4} \quad (30)$$

This results in $\sigma = 0.057$ C/m^2 (1 electron charge per 2.8 nm^2), which may be compared to $\sigma = 0.071$ C/m^2 in the case of no added polyelectrolyte. Most likely, the decreasing surface potential and charge on addition of HA arises from the adsorption of some positively charged Na^+ counterions of HA onto the negatively charged mica surfaces.

Equation 28 may also be applied to other studies in which big macroions were involved. As noted in the Introduction, the only such study we are aware of is that of Pashley and Ninham,[2] to be referred to as P−N, who used the SFA to measure the double-layer repulsion between two CTAB bilayers immersed in an ionic micellar solution (rather than polyelectrolyte). They calculated the effective Debye length κ_{eff}^{-1} by fitting their experimental data with a numerical solution of the nonlinear Poisson−Boltzmann equation. P−N proposed an empirical expression for κ_{eff}^{-1}, defined by

$$\kappa^{-1} = \left[\frac{\epsilon\epsilon_0 k_B T}{e^2(2n_s + Zn_p)}\right]^{1/2} = \frac{0.43}{\sqrt{2n_s + Zn_p}}\ \text{nm} \quad (31)$$

which they compared to their fitted experimental values. In eq 31, n_s and n_p refer to the molar concentrations of the free surfactant molecules (cmc) and the micelles, respectively, and Z is the number of elementary charges per micelle.[41] The results are shown in Table 1 below, together with our predictions using eq 28.

As seen in Table 1, our theoretical predictions are at least as good (even slightly better at the higher micelle concentrations) as the empirical expression of P−N, which is purely heuristic and was not theoretically derived. Note that only the two highest CTAB concentrations are significantly higher than the cmc of 9.7×10^{-4} M[42] and hence contain a considerable amount of micelles. We should also note that the range of distances used by P−N was mostly *larger* than the size of the micelles of ~3−4 nm,[43] and it is therefore not obvious whether the micelles and their counterions remained between the surfaces when the theories of Borukhov et al.[4,5] are expected to hold or whether the micelles were depleted from between the surfaces when eq 28 should hold. Probably, the actual physical situation is in between these two regimes—which may be one reason for the (small) discrepancies between our theoretical predictions and the experimental values.

It appears from our model and from comparing the model with our measurements that the only parameter that changes the Debye length is not the polyelectrolyte concentration per se, but the concentration of the small permeable counterions that dissociate from this polyelectrolyte into the solution, viz., Zn_p. This is provided that the polymer is sufficiently large compared to the gap between the surfaces when the assumption of no polymer between the surfaces, as used in our model, is valid.

Acknowledgment. We acknowledge Charles W. McCutchen for his comments on an earlier version of this manuscript. This work was supported by a grant from the McCutchen Foundation, and by the Materials Research Laboratory (MRL), under NSF Grants DMR00- 80034 and DMR 9972246.

Appendix. Minimization of the Grand Potential Functional

To obtain the equilibrium electrolyte distributions at all points within the gap between the surfaces, we need to minimize the grand potential with respect to the

Table 1. Comparison of Eq 28 with P−N Study[2] on Micellar Solutions

measured values (P−N experiment[2])				calculated Debye lengths, κ_{eff}^{-1} (nm), based on $Z = 12.5$ (ref 41)	
total surfactant concn[a] [CTAB], M	monomer concn[a] n_s (M)	micelle concn[a] n_p (M)	Debye length, κ_{eff}^{-1} (nm)	P−N empirical, eq 31	present theory, eq 28
10^{-3}	9.7×10^{-4}	6.0×10^{-7}	10.0	9.5	9.7
2×10^{-3}	9.7×10^{-4}	2.1×10^{-5}	8.5	8.9	9.2
5×10^{-3}	9.7×10^{-4}	8.1×10^{-5}	7.8	7.9	8.2
10^{-2}	9.7×10^{-4}	1.81×10^{-4}	7.0	6.6	7.2
1.8×10^{-2}	9.7×10^{-4}	3.41×10^{-4}	6.0	5.4	6.4

[a] Note that the total surfactant concentration [CTAB] in column 1 includes both the free CTAB monomers in solution at the critical micelle concentration (cmc) of $n_s = 9.7 \times 10^{-4}$ M (ref 42) and the CTAB molecules in micelles.

distributions of all the ions subject to the restriction of global charge neutrality, eq 10, that is

$$\frac{\delta}{\delta n_c(X)}\left[\frac{\Omega}{2Ak_BT}\right] = \lambda \frac{\delta F}{\delta n_c(X)} \quad \text{and} \quad \frac{\delta}{\delta n_s(X)}\left[\frac{\Omega}{2Ak_BT}\right] = \lambda \frac{\delta F}{\delta n_s(X)} \quad \text{(A1)}$$

This leads to eq 11, which we now derive from eq 9. First, we rewrite eq 9 as

$$\frac{\Omega}{2Ak_BT} = \int_0^{D/2} dX \left\{ n_c(X) \ln[n_c(X)/n_c] + n_s(X) \ln[n_s(X)/n_s] - \left[n_c(X) + n_s(X) - \frac{\Pi_0}{k_BT} \right] \right\} + \frac{\Omega_{electr}}{2Ak_BT} \quad \text{(A2)}$$

where $\Omega_{electr}/2Ak_BT \equiv {}^1/_2\int_0^{D/2} dX \{\phi(X)[n_c(X) - n_s(X) - \sigma\delta(X)]\}$. Because of the symmetry of the system around $D/2$, the integral from 0 to $D/2$ is half of the integral to D (including a term in the integrand that takes into account the charge on the surface at $X = D$). Thus

$$\frac{\Omega_{electr}}{2Ak_BT} = \frac{1}{4}\int_0^D dX \{\phi(X)[n_c(X) - n_s(X) - \sigma\delta(X) - \sigma\delta(X - D)]\} \quad \text{(A3)}$$

Substituting eq 7 for the electrostatic potential, we get after rearranging

$$\frac{\Omega_{electr}}{2Ak_BT} = -\left(\frac{2e^2}{\epsilon\epsilon_0 k_BT}\right)\frac{1}{4}\int_0^D\int_0^D dX\, dX' \times [n_c(X') - n_s(X') - \sigma\delta(X') - \sigma\delta(X' - D)] \times [n_c(X) - n_s(X) - \sigma\delta(X) - \sigma\delta(X - D)]|X - X'|\} \quad \text{(A4)}$$

To minimize the whole grand potential, we need its functional variation with respect to both electrolyte distributions, $n_s(X)$ and $n_c(X)$. First we calculate the functional variation of the electrostatic part of the grand potential which, taking into account the symmetry of the integrand with respect to the variables X and X', results in

$$\delta\left[\frac{\Omega_{electr}}{2Ak_BT}\right] = -\left(\frac{2e^2}{\epsilon\epsilon_0 k_BT}\right)\frac{1}{2}\int_0^D\int_0^D dX\, dX' |X - X'| \times \{[\delta n_c(X) - \delta n_s(X)][n_c(X') - n_s(X') - \sigma\delta(X') - \sigma\delta(X' - D)] \quad \text{(A5)}$$

Rearranging and using eq 7, we get

$$\delta\left[\frac{\Omega_{electr}}{2Ak_BT}\right] = \frac{1}{2}\int_0^D dX\, [\delta n_c(X) - \delta n_s(X)]\phi(X) = \int_0^{D/2} dX\, [\delta n_c(X) - \delta n_s(X)]\phi(X) \quad \text{(A6)}$$

Equation A6 is the expression for the functional variation of the electrostatic part of the grand potential. To calculate the functional variation of the whole grand potential, we differentiate eq A2 which results in

$$\delta\left[\frac{\Omega}{2Ak_BT}\right] = \int_0^{D/2} dX \{\delta n_c(X) \ln[n_c(X)/n_c] + \delta n_c(X) + \delta n_s(X) \ln[n_s(X)/n_s] + \delta n_s(X) - [\delta n_c(X) + \delta n_s(X)]\} + \delta\left[\frac{\Omega_{electr}}{2Ak_BT}\right] \quad \text{(A7)}$$

The minimization of the grand potential is obtained by substituting eqs 10, A6, and A7 into eq A1, which leads to

$$\delta\left[\frac{\Omega}{2Ak_BT}\right] = \int_0^{D/2} dX \{\delta n_c(X) \ln[n_c(X)/n_c] + \delta n_s(X) \ln[n_s(X)/n_s] + [\delta n_c(X) - \delta n_s(X)]\phi(X)\} = \lambda\delta F = \lambda\int_0^{D/2}[\delta n_c(X) - \delta n_s(X)]\, dX \quad \text{(A8)}$$

Since $\delta n_c(X)$and $\delta n_s(X)$ are independent of each other, and of $\delta n_c(X)$ and $\delta n_s(X')$ for $X \neq X'$, each of the square brackets should be zero, which finally leads to eq 11.

References and Notes

(1) Mondainmonval, O.; Lealcalderon, F.; Phillip, J.; Bibette, J. *Phys. Rev. Lett.* **1995**, *75*, 3364−3367.
(2) Pashley, R. M.; Ninham, B. W. *J. Phys. Chem.* **1987**, *91*, 2902−2904.
(3) Richetti, P.; Kekicheff, P. *Phys. Rev. Lett.* **1992**, *68*, 1951−1954.
(4) Borukhov, I.; Andelman, D.; Orland, H. *Phys. Rev. Lett.* **1997**, *79*, 435−438.
(5) Borukhov, I.; Andelman, D.; Orland, H. *Electrochim. Acta* **2000**, *46*, 221−229.
(6) Borukhov, I.; Andelman, D.; Orland, H. *Europhys. Lett.* **1995**, *32*, 499−504.
(7) Fouissac, E.; Milas, M.; Rinaudo, M. *Macromolecules* **1993**, *26*, 6945−6951.
(8) Tadmor, R.; Chen, N.; Israelachvili, J. N. *J. Biomed. Mater. Res.*, in press (2002).
(9) Armstrong, D. C.; Johns, M. R. *Appl. Environ. Microbiol.* **1997**, *63*, 2759−2764.
(10) Israelachvili, J. N.; McGuiggan, P. *J. Mater. Res.* **1990**, *5*, 2223−2231.
(11) Israelachvili, J. N.; Adams, G. E. *J. Chem. Soc., Faraday Trans. 1* **1978**, *74*, 975−1001.
(12) Israelachvili, J. N. *J. Colloid Interface Sci.* **1973**, *44*, 259−272.
(13) Derjaguin, B. V. *Kolloid Zh.* **1934**, *69*, 155−164.
(14) Tsutsumi, K.; Norisuye, T. *Polym. J.* **1998**, *30*, 345−349.
(15) Van Krevelen, D. W. *Properties of Polymers*, 3rd ed.; Elsevier Science B.V.: Amsterdam, 2000.
(16) Taunton, H. J.; Toprakcioglu, C.; Fetters, L. J.; Klein, J. *Macromolecules* **1990**, *23*, 571−580.
(17) Janik, J.; Tadmor, R.; Klein, J. *Langmuir* **1997**, *13*, 4466−4473.
(18) Ruths, M.; Steinberg, S.; Israelachvili, J. N. *Langmuir* **1996**, *12*, 6637−6650.
(19) Israelachvili, J. N. *J. Colloid Interface Sci.* **1986**, *110*, 263−271.
(20) Verwey, E. J. W.; Overbeek, J. T. G. *Theory of the Stability of Lyophobic Colloids*; Dover: New York, 1948.
(21) Israelachvili, J. N. *Intermolecular & Surface Forces*, 2nd ed.; Academic Press: London, 1991.
(22) Grahame, D. C. *Chem. Rev.* **1947**, *41*, 441−501.
(23) Dubois, M.; Zemb, T.; Belloni, L.; Delville, A.; Levitz, P.; Setton, R. *J. Chem. Phys.* **1992**, *96*, 2278−2286.
(24) If the charged particles were point charges, with a concentration n_p and a net charge of $Q = Z_p e$ per particle (Z_p electronic charges), their contribution to $\sum n_i z_i^2$ in eq 4a for the Debye length should involve a term $n_p Z_p^2$ from the particles and another term $n_p Z_p$ from the counterions (which are assumed to be monovalent). For large Z_p this contribution can be large even when n_p is small, but it is generally neglected in the calculation of the Debye length of a colloidal system.
(25) Assuming a projection of 1.25 Å per each interatomic bond along the chain, we obtain 16.25 Å between two adjacent charges. This number is exaggerated for two reasons: it does not take into account the additional entropic bending of the

chain (this is a small effect for the rather short 13 chemical bonds), and it does not take into account the association of two or more HA molecules as shown by Scott et al. (refs 26 and 28). However, apparently the value is still larger than 7 Å (the Bjerrum length) since even Scott et al. assumed in their calculations fully dissociated HA (ref 27, Table 2). The degree of dissociation of a linear polyelectrolyte is generally less than 100% due to Manning condensation (refs 32−35) and could in principle be determined from osmotic pressure data (ref 31); however, the theories in this field (see, for example, refs 29 and 30), though beneficial for determining trends, are not yet sufficiently developed to give accurate quantitative values.

(26) Heatley, F.; Scott, J. E. *Biochem. J.* **1988**, *254*, 489−493.
(27) Scott, J. E.; Chen, Y.; Brass, A. *Eur. J. Biochem.* **1992**, *209*, 675−680.
(28) Scott, J. E.; Heatley, F.; Hull, W. E. *Biochem. J.* **1984**, *220*, 197−205.
(29) Wang, L. X.; Bloomfield, V. A. *Macromolecules* **1990**, *23*, 194−199.
(30) Wang, L. X.; Bloomfield, V. A. *Macromolecules* **1990**, *23*, 804−809.
(31) Laurent, T. C.; Ogston, A. G. *Biochem. J.* **1963**, *89*, 249−253.
(32) Manning, G. S. *J. Chem. Phys.* **1969**, *51*, 924−933.
(33) Manning, G. S. *Ber. Bunsen-Ges. Phys. Chem.* **1996**, *100*, 909−922.
(34) Manning, G. S. *Physica A* **1996**, *231*, 236−253.
(35) Manning, G. S.; Ray, J. *J. Biomol. Struct. Dyn.* **1998**, *16*, 461−476.
(36) Callen, H. B. *Thermodynamics and an Introduction to Thermostatistics*, 2nd ed.; Wiley: New York, 1985.
(37) Safran, S. A. *Statistical Thermodynamics of Surfaces, Interfaces, and Membranes*; Addison-Wesley: Reading, MA, 1994.
(38) Andelman, D. In *Handbook of Biological Physics*; Lipowsky, R., Sackmann, E., Eds.; Elsevier: Amsterdam, 1995; Vol. 1B.
(39) Honig, E. P.; Mul, P. M. *J. Colloid Interface Sci.* **1971**, *36*, 258−272.
(40) White, L. R. *J. Colloid Interface Sci.* **1983**, *95*, 286−288.
(41) P−N assumed 50 surfactant molecules per micelle, of which 25% are dissociated. This gives $Z = 12.5$.
(42) Blandamer, M. J.; Cullis, P. M.; Soldi, L. G.; Rao, K. C.; Subha, M. C. S. *J. Therm. Anal.* **1996**, *46*, 1583−1588.
(43) Adamson, A. W.; Gast, A. P. *Physical Chemistry of Surfaces*; John Wiley: New York, 1997.

MA011893Y